Nonlinear eigenvalue problems and *PT*-symmetric quantum mechanics

IOP Conf. Series: Journal of Physics: Conf. Series **873** (2017) 012002 doi:10.1088/1742-6596/873/1/012002

Nonlinear eigenvalue problems and $\mathcal{PT}$-symmetric quantum mechanics

Carl M. Bender

Department of Physics, Washington University, St. Louis, MO 63130, USA

E-mail: cmb@wustl.edu

Abstract. Semiclassical (WKB) techniques are commonly used to find the large-energy behavior of the eigenvalues of linear time-independent Schrödinger equations. In this talk we generalize the concept of an eigenvalue problem to nonlinear differential equations. The role of an eigenfunction is now played by a separatrix curve, and the special initial condition that gives rise to the separatrix curve is the eigenvalue. The Painlevé transcendents are examples of nonlinear eigenvalue problems, and semiclassical techniques are devised to calculate the behavior of the large eigenvalues. This behavior is found by reducing the Painlevé equation to the linear Schrödinger equation associated with a non-Hermitian $\mathcal{PT}$-symmetric Hamiltonian. The concept of a nonlinear eigenvalue problem extends far beyond the Painlevé equations to huge classes of nonlinear differential equations.

1. Introduction

This talk is focused on the notion of *stability*. We begin by reviewing the concept of $\mathcal{PT}$-symmetric quantum theory, and we show that $\mathcal{PT}$-symmetric systems that appear unstable may actually be stable because they are defined in a complex domain rather than a real domain. Next, we explain that stability (and instability) plays a crucial role in a conventional Schrödinger eigenvalue problem. (A small perturbation of an eigenvalue prevents the boundary conditions from being satisfied.) We then introduce the idea of a *nonlinear* eigenvalue problem in the context of an elementary example and show that the concepts of stability and eigenvalues are intimately linked. Finally, we consider some sophisticated nonlinear eigenvalue problems for the Painlevé transcendents and show that there is a connection between $\mathcal{PT}$-symmetric Hamiltonians and the Painlevé transcendents. Finally, we discuss eigenvalue problems that are posed for nonlinear equations beyond the Painlevé class of differential equations.

2. Brief review of $\mathcal{PT}$-symmetric quantum theory

In the DISCRETE2014 conference in London I presented a talk introducing the ideas of $\mathcal{PT}$-symmetric quantum theory [1]. In that talk I explained that in $\mathcal{PT}$-symmetric quantum theory the mathematical condition of Hermiticity, where the adjoint † represents combined complex conjugation and matrix transposition, is replaced by the weaker and more physical condition of $\mathcal{PT}$ symmetry (invariance under space-time reflection). Here, $\mathcal{P}$ is the space reflection operator, $\mathcal{P}: x \to -x, p \to -p$, and $\mathcal{T}$ is the time reversal operator $\mathcal{T}: x \to x, p \to -p, i \to -i$. Invariance under $\mathcal{PT}$ reflection is a physical condition because $\mathcal{P}$ and $\mathcal{T}$ are elements of the Lorentz group [2, 3]. Many laboratory studies of $\mathcal{PT}$-symmetric models

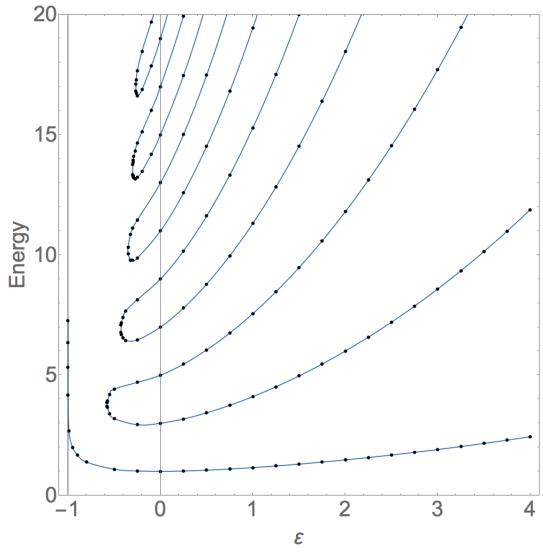

Figure 1. Real eigenvalues of the Hamiltonian $H = p^2 + x^2(ix)^\varepsilon$ plotted as functions of the parameter ε. In the region of *unbroken* $\mathcal{PT}$ *symmetry* $\varepsilon \geq 0$ the spectrum is real, positive, and discrete. However, in the region of *broken* $\mathcal{PT}$ *symmetry* $\varepsilon < 0$, the real eigenvalues merge pairwise and form complex-conjugate pairs. When $-1 < \varepsilon < 0$, there are a finite number of real positive eigenvalues and an infinite number of complex-conjugate pairs of eigenvalues. When $\varepsilon \leq -0.57793$, there is just one real eigenvalue, and as $\varepsilon \to -1^+$ this real eigenvalue becomes infinite.

have been published. These experiments have been performed in such diverse areas as optics [4, 5, 6, 7, 8, 9, 10, 11, 12, 13, 14, 15, 16], nuclear magnetic resonance [17], superconductivity [18, 19], microwave cavities [20, 21], laser physics [22, 23], atomic diffusion [24], electronic and mechanical systems [26, 27, 28, 29], optical graphene [30, 31], optical resonators [32, 33, 34], Bose-Einstein condensates [35, 36, 37], and metamaterials [38, 39, 40, 41].

A heavily studied one-parameter family of $\mathcal{PT}$-symmetric Hamiltonians is

$$H = p^2 + x^2(ix)^\varepsilon, \tag{1}$$

and the eigenvalues of this Hamiltonian are shown in Fig. 1. A proof that the eigenvalues of H are real was first given by Dorey, Dunning, and Tateo [42, 43]. Two special cases of H in (1) are

$$H = p^2 + ix^3 \quad \text{and} \quad H = p^2 - x^4, \tag{2}$$

which are obtained when $\varepsilon = 1$ and $\varepsilon = 2$. The latter Hamiltonian has an upside-down potential, and thus appears to be unstable. Nevertheless, it has bound states at *positive* discrete energies (see Fig. 1). The stability of this Hamiltonian has been established rigorously [44, 45].

A heuristic explanation for why an upside-down potential, such as that in (2), may be stable is that a $\mathcal{PT}$-symmetric quantum theory is an extension (an analytic continuation) of a conventional quantum theory into the complex plane. [The Hamiltonian H in (1) is an analytic continuation in ε of the conventional quantum-harmonic-oscillator Hamiltonian $p^2 + x^2$.] When we use the term *unbounded*, we mean that the energy is unbounded below. However, the complex numbers are not ordered, so the notions of $>$ (greater than) and $<$ (less than) do not apply. Thus, it is not obvious which complex potentials have bound states and which do not. One must distinguish between these two possibilities to determine if a system is stable.

The stability of a negative quartic potential has implications in quantum field theory. For example, the double-scaling limit of a O(N)-symmetric quartic scalar field theory appears flawed because an upside-down potential arises in that limit. However, this limit is perfectly acceptable as a $\mathcal{PT}$-symmetric theory [46, 47]. In quantum field theory the process of renormalization can introduce instabilities by making the Hamiltonian non-Hermitian. For example, for the Lee Model [48], Källén and Pauli showed that renormalization introduces non-Hermiticity, which appears to make the scattering matrix nonunitary and leads to ghost states [49]. The techniques of $\mathcal{PT}$-symmetric quantum theory fully resolve these problems [50]. Similarly, renormalization

introduces non-Hermiticity in the Standard Model, which appears to make the Higgs vacuum state unstable. Again, $\mathcal{PT}$-symmetry resolves this problem [51]. This stabilization effect works at the classical level as well. An example of a classical instability is the runaway mode in the electromagnetic self-force problem. $\mathcal{PT}$-symmetric analysis resolves this problem [52].

The purpose of this paper is to examine the instabilities that arise in eigenvalue problems associated with classical nonlinear differential equations, and in particular the Painlevé transcendents. We will demonstrate that $\mathcal{PT}$ symmetry resolves these instabilities. Indeed, we will show that there is a deep connection between the Painlevé transcendents and the class of Hamiltonians in (1). To do so we will generalize the notion of an eigenvalue problem for a linear differential equation to an eigenvalue problem for a nonlinear differential equation. In the nonlinear context a separatrix plays the role of an eigenfunction and the initial conditions that give rise to the separatrix play the role of the eigenvalues.

3. Instabilities associated with eigenvalue problems

In quantum mechanics the eigenvalue problems for the linear second-order time-independent Schrödinger equation are well understood. This equation has the form

$$-y''(x) + V(x)y(x) = Ey(x), \tag{3}$$

where E is the eigenvalue. For a rising potential $V(x)$ the eigenfunction $y(x)$ is required to satisfy homogeneous boundary conditions at $\pm\infty$: $y(-\infty) = 0$, $y(\infty) = 0$. Semiclassical (WKB) techniques give accurate approximations to the large eigenvalues. The leading WKB approximation to the nth eigenvalue E_n is given by the phase-integral condition

$$\int_{x_{\rm L}}^{x_{\rm R}} dx\sqrt{E_n - V(x)} \sim \left(n + \tfrac{1}{2}\right)\pi \quad (n \gg 1), \tag{4}$$

where $x = x_{\rm L}$ and $x = x_{\rm R}$ are turning points that satisfy the equation $V(x) = E_n$. Typically, the semiclassical (high-energy) approximation to E_n has the form $E_n \sim ab^n \quad (n \gg 1)$, where a and b are determined by the condition (4). For example, the semiclassical approximation to the eigenvalues of the harmonic oscillator $V(x) = x^2$ is $E_n \sim 2n$ $(n \gg 1)$, and for the anharmonic oscillator $V(x) = x^4$ we get $E_n \sim [3\Gamma(3/4)\sqrt{\pi}/\Gamma(1/4)]^{4/3}\, n^{4/3}$ $(n \gg 1)$.

The solutions to the linear eigenvalue problem (3) have characteristic qualitative features. If $V(x)$ has a single minimum and rises as $x \to \pm\infty$ (like the potentials x^2 and x^4), the eigenfunctions exhibit distinct behaviors in each of five regions of x: When $x > x_{\rm R}$ and when $x < x_{\rm L}$, the eigenfunctions $y_n(x)$ decay exponentially as $|x| \to \infty$; these are the *classically forbidden* regions. However, when $x_{\rm L} < x < x_{\rm R}$, the eigenfunctions are oscillatory and $y_n(x)$ has exactly n nodes; this is the *classically allowed* region. Near $x_{\rm L}$ and $x_{\rm R}$, there is a transition between exponentially decreasing and oscillatory behavior, which is universally described by the Airy function $\mathrm{Ai}(x)$. Furthermore, the eigenfunctions exhibit unstable behavior: There is an abrupt change in the character of the solution to (3) as E moves away from an eigenvalue; an infinitesimal change in E away from an eigenvalue causes the eigenfunction to lose the property of square integrability. This is the instability referred to earlier.

Nonlinear differential equations can have eigenfunction-like solutions whose behaviors are strongly analogous to the behaviors of eigenfunctions for linear eigenvalue problems. This idea was originally proposed and investigated in Ref. [53]. It was shown that *a nonlinear differential equation may have a discrete set of critical initial conditions that give rise to unstable separatrix solutions.* We treat these initial conditions as *eigenvalues* and the unstable separatrices that come from these special initial conditions as the corresponding *eigenfunctions.* Our objective here will be to find the large-n (semiclassical) asymptotic behavior of the nth eigenvalue by using both numerical and analytic techniques.

A simple-looking first-order nonlinear differential equation that exhibits eigenfunction and eigenvalue behavior is

$$y'(x) = \cos[\pi x y(x)] \tag{5}$$

with the initial condition $y(0) = E$. The initial value E plays the role of an eigenvalue. Solutions to this equation for various initial conditions E are plotted in Fig. 2.

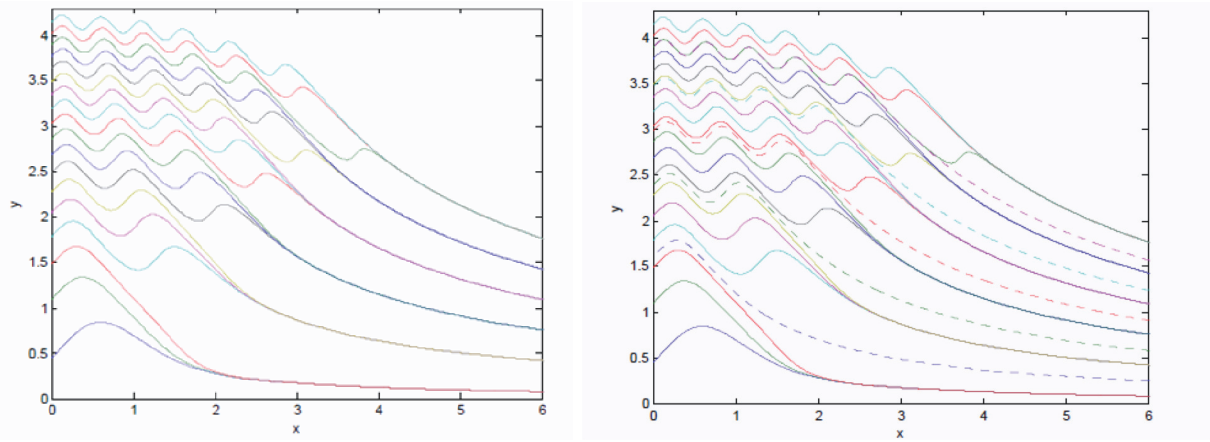

Figure 2. Left panel: Numerical solutions $y(x)$ to (5) for $0 \leq x \leq 6$ with initial conditions $y(0)$ ranging from 0 to 4.2. The solutions initially oscillate but abruptly change their character and decay smoothly and monotonically. In the decaying regime solutions merge into quantized bundles and the bundles decay like $1/x$ as $x \to \infty$. Right panel: Same as left panel except that the separatrix (eigenfunction) solutions (dashed lines) to (5) are shown. The separatrix solutions begin at the eigenvalues $E_1 = 1.6026$, $E_2 = 2.3884$, $E_3 = 2.9767$, $E_4 = 3.4675$, and $E_5 = 3.8975$. The separatrices are unstable; if $y(0)$ lies infinitesimally below (above) the eigenvalue, the solution rapidly diverges away from the separatrix and merges with the bundle of solutions below (above) the separatrix.

Figure 2 shows that solutions to the initial-value problem (5) have n maxima before vanishing like $1/t$ as $t \to \infty$. As the initial condition $y(0)$ increases past the special critical value E_n, the number of maxima changes from n to $n+1$. At these critical values the solution $y(t)$ to (5) is an unstable separatrix curve. We understand this instability as follows: If $y(0)$ lies infinitesimally below E_n, the solution merges with a bundle of stable solutions all having n maxima, and when $y(0)$ is infinitesimally above E_n, the solution merges with a bundle of stable solutions all having $n+1$ maxima. The separatrix curves are displayed in Fig. 2 (right panel) as dashed curves.

The nonlinear eigenvalue problem illustrated in Fig. 2 is qualitatively similar to the linear eigenvalue problem (3) for the time-independent Schrödinger equation. First, the separatrices are unstable with respect to a small change in the eigenvalue E_n; if $y(0) = E_n$ is increased or decreased slightly, $y(x)$ abruptly jumps from the asymptotic bundle of solutions on one side of the separatrix to the asymptotic bundle on the other side of the separatrix. Also, the eigenfunctions (separatrix curves) corresponding to the nth eigenvalue (the initial condition E_n) exhibit n oscillations in the analog of a classically allowed region before decreasing monotonically to 0 in the analog of a classically forbidden region. We can see in Fig 2 that this change from oscillatory to decaying behavior occurs over a narrow region that is the analog of a turning-point region.

An exact formula for the nth eigenvalue E_n is unknown, and without such a formula our objective is to determine the asymptotic behavior of the critical values E_n for large n. It was shown in Ref. [53] that for large n the nonlinear-differential-equation problem (5) reduces to a

linear one-dimensional random-walk problem. This random-walk problem was solved exactly and it was thereby established analytically that the nth eigenvalue grows like an^b for large n:

$$E_n \sim 2^{5/6}\sqrt{n} \quad (n \to \infty). \tag{6}$$

Kerr found an alternative derivation of this remarkable semiclassical (high-energy) solution to this asymptotics problem and verified (6) [54]. [The numerical constant $a = 2^{5/6}$ and the exponent $b = 1/2$ are remarkable because there is no hint of such numbers in (5)!]

There is a huge class of *second-order* nonlinear differential-equation eigenvalue problems having discrete eigenvalues. In Refs. [53, 55] it was shown that the first two Painlevé transcendents lead to eigenvalue problems. (These are discussed in Sec. 4.) The Painlevé equations have the special property that their solutions have *movable* (*spontaneous*) singularities that are poles. There are no other kinds of movable singularities, such as branch points. Thus, the solutions to these differential equations are *meromorphic* (defined on a one-sheeted Riemann surface) and such solutions are readily studied by using numerical and asymptotic analysis. The large-eigenvalue behaviors of these equations can be found asymtotically by linearizing the eigenvalue problems. Specifically, for large n the nonlinear eigenvalues are approximated by the eigenvalues of a *linear* Schrödinger eigenvalue problem and the Hamiltonian for this problem belongs to the class of $\mathcal{PT}$-symmetric non-Hermitian Hamiltonians (1) [2].

In Ref. [55] it was proposed that one could extend the study of nonlinear-differential-equation eigenvalue problems beyond the Painlevé transcendents to more complicated differential equations such as the Thomas-Fermi equation $y''(x) = [y(x)]^{3/2}x^{1/2}$, and clearly the physical solution to this equation, which satisfies the boundary conditions $y(0) = 1$ and $y(+\infty) = 0$, is an eigenfunction solution. Like the solutions to (5), $y(x)$ vanishes algebraically (like $144x^{-3}$) as $x \to \infty$. This is an unstable separatrix solution and the specific value of $y'(0)$ that gives rise to this solution is an eigenvalue. If $y'(0)$ is larger than the critical value of $y'(0)$, the function $y(x)$ becomes singular at some point $x = a$ and blows up like $400a(x-a)^{-4}$ as $x \to a$; if $y'(0)$ is less than the critical value, the function $y(x)$ crosses 0 and becomes complex. Unfortunately, the movable singularity at $x = a$ is a *logarithmic branch-point* singularity [to verify this one must expand $y(x)$ to sixteenth order in powers of $(x-a)$] and therefore the solutions to this equation live on a Riemann surface having infinitely many sheets. Thus, for this equation it is not easy to find additional separatrix solutions.

However, we have found infinite numbers of nonlinear differential equations whose movable singularities are *algebraic* branch points, and these equations, which are discussed in Sec. 5, are analytically tractable. The features of these new kinds of nonlinear differential-eigenvalue problems are qualitatively similar to those of the Painlevé equations [56].

4. Instabilities associated with the Painlevé transcendents

The Painlevé transcendents are six second-order nonlinear differential equations whose movable (spontaneous) singularities are poles (and not branch points, essential singularities, or other kinds of singularities). Many papers and books have been written on these beautiful differential equations [57, 58, 59, 60, 61, 62, 63, 64] and these equations arise often in mathematical physics [65, 66, 67, 68, 69, 70, 71].

This section is focused mostly on the first and second Painlevé transcendents, referred to here as PI and PII. The initial-value problem (IVP) for the PI differential equation is

$$y''(t) = 6[y(t)]^2 + t, \qquad y(0) = c,\ y'(0) = b \tag{7}$$

and the IVP for PII (in which an arbitrary additive constant is set to 0) is

$$y''(t) = 2[y(t)]^3 + ty(t), \qquad y(0) = c,\ y'(0) = b. \tag{8}$$

For the fixed initial condition $y(0) = 0$ there is a discrete set of initial slopes $y'(0) = b_n$ that give rise to unstable separatrix solutions. Similarly, for fixed initial slope $y'(0) = 0$, there is a discrete set of initial values $y(0) = c_n$ that give rise to separatrix solutions. For Painlevé I the large-n asymptotic behavior of the eigenvalues b_n and c_n is

$$b_n \sim B_{\rm I} n^{3/5} \quad (n \to \infty) \quad \text{and} \quad c_n \sim C_{\rm I} n^{2/5} \quad (n \to \infty). \tag{9}$$

For Painlevé II the large-n asymptotic behavior of the eigenvalues b_n and c_n are

$$b_n \sim B_{\rm II} n^{2/3} \quad (n \to \infty) \quad \text{and} \quad c_n \sim C_{\rm II} n^{1/3} \quad (n \to \infty). \tag{10}$$

We have determined the coefficients $B_{\rm I}$, $C_{\rm I}$, $B_{\rm II}$, and $C_{\rm II}$ in these asymptotic behaviors analytically and numerically. The analytical calculation of these constants for PI and PII is done by reducing the nonlinear equations to the linear eigenvalue problems for the cubic and quartic $\mathcal{PT}$-symmetric Hamiltonians $H = \frac{1}{2}p^2 + 2ix^3$ and $H = \frac{1}{2}p^2 - \frac{1}{2}x^4$ [44] [see (2)].

Let us look at the PI equation. In Ref. [72] there is a brief asymptotic study of the first Painlevé transcendent (7). One can easily show that there are two possible asymptotic behaviors of the solution to this differential equation as $t \to -\infty$; the solutions can approach either $+\sqrt{-t/6}$ or $-\sqrt{-t/6}$. If the solution $y(t)$ approaches $-\sqrt{-t/6}$, the solution oscillates *stably* about this curve with gradually decreasing amplitude. However, while the curve $+\sqrt{-t/6}$ is another possible asymptotic behavior, this behavior is *unstable* and *nearby solutions tend to veer away from it.* The eigenfunctions of PI are those solutions that *do* approach the curve $+\sqrt{-t/6}$ as $t \to -\infty$. These separatrix solutions resemble the eigenfunctions of conventional quantum mechanics in that they exhibit n oscillations before settling down to this asymptotic behavior. However, because the PI equation is nonlinear, these oscillations are unbounded; the nth eigenfunction passes through $[n/2]$ double poles where it blows up, and only then does it smoothly approach the curve $+\sqrt{-t/6}$. (The symbol $[n/2]$ means greatest integer in $n/2$.)

To find the numerical solutions to the initial-value problem for the PI equation (7) for $t < 0$ we use Runge-Kutta to integrate down the negative-real axis. When we approach a double pole and the solution becomes large and positive, we estimate the location of the pole and integrate along a semicircle in the complex-t plane around the pole. We then continue integrating down the negative-real axis. We begin by choosing the fixed initial value $y(0) = 0$ and allow the initial slope $y'(0) = b$ to have increasingly positive values. (We only present results for positive initial slope; the behavior for negative initial slope is analogous.) We find that the particular choice of $y(0)$ is not crucial and that for *any* fixed $y(0)$ the large-n leading asymptotic behavior of the initial-slope eigenvalues b_n is the same.

Above the critical value $b_1 = 1.851854034$ (first eigenvalue) there is a continuous interval of b for which $y(t)$ first has a minimum and then has an infinite sequence of double poles (Fig. 3, left panel). However, if b increases past the next critical value $b_2 = 3.004031103$ (second eigenvalue), the character of the solutions changes abruptly and $y(t)$ oscillates stably about $-\sqrt{-t/6}$ (Fig. 3, right panel). When b exceeds the critical value $b_3 = 3.905175320$ (third eigenvalue), the solutions again exhibit an infinite sequence of poles (Fig. 4, left panel). When b increases past the fourth critical value $b_4 = 4.683412410$ (fourth eigenvalue), the solutions once again oscillate stably about $-\sqrt{-t/6}$ (Fig. 4, right panel). There is an infinite sequence of critical points (eigenvalues) at which the PI solutions alternate between infinite sequences of double poles and stable oscillation about $-\sqrt{-t/6}$.

The separatrix (eigenfunction) solutions that arise when $y'(0)$ is an eigenvalue have a completely different (and unstable) character from those in Figs. 3 and 4. These special solutions exhibit a *finite* number $[n/2]$ of double poles (analogous to the oscillatory behavior of quantum-mechanical bound-state eigenfunctions in the classically allowed region of a potential well) and then exhibit a turning-point-like transition in which the poles abruptly cease and $y(t)$

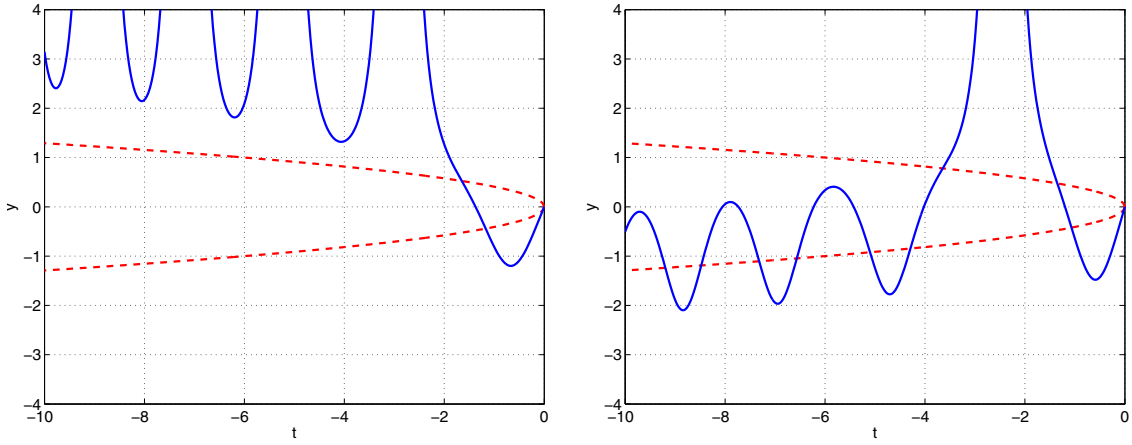

Figure 3. Typical behavior of solutions to the first Painlevé transcendent $y(t)$ for the initial conditions $y(0) = 0$ and $b = y'(0)$. Left panel:$b = 2.504031103$, which lies between the eigenvalues $b_1 = 1.851854034$ and $b_2 = 3.004031103$. Right panel: $b = 3.504031103$, which lies between the eigenvalues $b_2 = 3.004031103$ and $b_3 = 3.905175320$. The dashed curves are $y = \pm\sqrt{-t/6}$. In the left panel the solution $y(t)$ has an infinite sequence of double poles and in the right panel the solution oscillates stably about $-\sqrt{t/6}$.

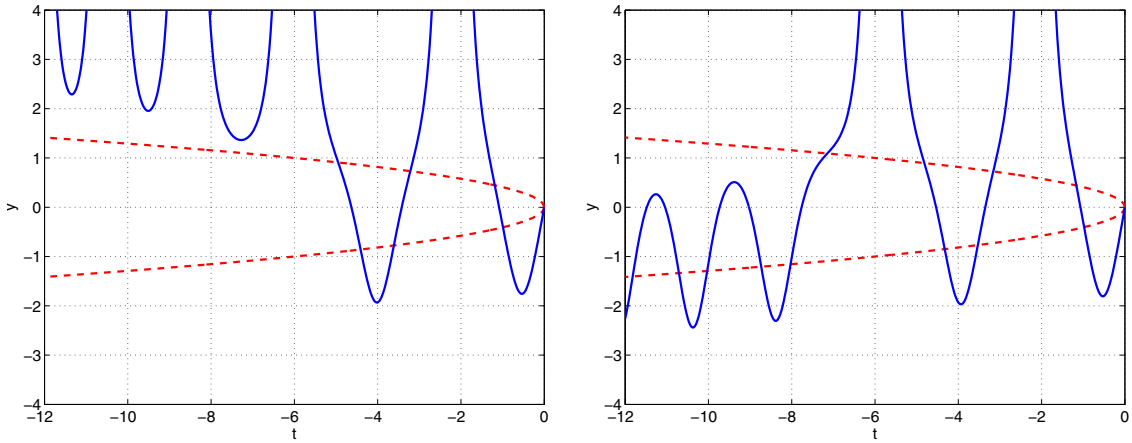

Figure 4. Solutions to the PI equation (7) for $y(0) = 0$ and $b = y'(0)$. Left panel: $b = 4.583412410$ (between the eigenvalues $b_3 = 3.905175320$ and $b_4 = 4.6834124103$). Right panel: $b = 4.783412410$ (between the eigenvalues $b_4 = 4.683412410$ and $b_5 = 5.383086722$).

exponentially decays towards the limiting curve $+\sqrt{-t/6}$. The solutions arising from the first and second critical points b_1 and b_2 are shown in Fig. 5, those arising from the third and fourth critical points b_3 and b_4 are shown in Fig. 6, and those arising from the tenth and eleventh critical points b_{10} and b_{11} are shown in Fig. 7. The critical points are analogous to eigenvalues because they give rise to *unstable* separatrix solutions; if $y'(0)$ changes by an infinitesimal amount above or below a critical value, the character of the solutions changes abruptly and the solutions exhibit the two possible kinds of generic behaviors shown in Figs. 3 and 4.

In Ref. [55] the constant $B_{\rm I}$ was determined numerically to great accuracy by applying fifth-order Richardson extrapolation to the first eleven eigenvalues. The value of $B_{\rm I}$ in (9) was found to an accuracy of one part in nine decimal places: $B_{\rm I} = 2.09214674$. The underlined digit lies in the range from 3 to 5 and $B_{\rm I}$ is accurate to one part in 2×10^8.

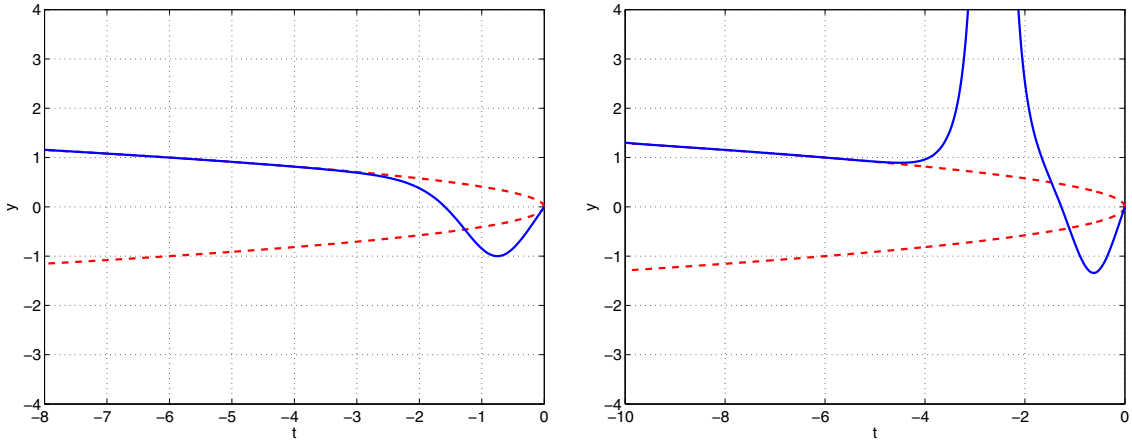

Figure 5. First two separatrix solutions (eigenfunctions) of Painlevé I with initial condition $y(0) = 0$. Left panel: $y'(0) = b_1 = 1.851854034$. Right panel: $y'(0) = b_2 = 3.004031103$. The dashed curves are $y = \pm\sqrt{-t/6}$.

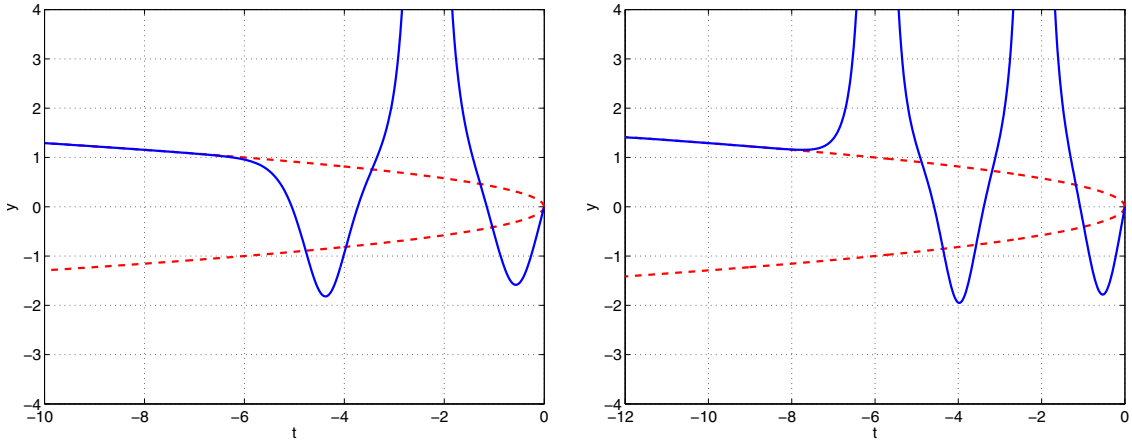

Figure 6. Third and fourth eigenfunctions of Painlevé I with initial condition $y(0) = 0$. Left panel: $y'(0) = b_3 = 3.905175320$. Right panel: $y'(0) = b_4 = 4.683412410$.

If the initial slope is held fixed at $y'(0) = 0$ and the initial value $y(0) = c$ is allowed to become increasingly negative, a new sequence of negative eigenvalues c_n appears for which the solutions resemble the eigenfunction separatrix solutions in Figs. 5–7. Fourth-order Richardson extrapolation applied to the first 15 eigenvalues reveals that for large n the sequence of initial-value eigenvalues c_n is asymptotic to $C_{\rm I} n^{2/5}$, where the constant $C_{\rm I}$ in (9) is $C_{\rm I} = -1.0304844$ (see Ref. [55]). The last digit is accurate to an error of ± 1 so $C_{\rm I}$ is determined to one part in 10^7. We have done similar numerical studies for PII and PIV, but to save space we do not repeat them here.

Asymptotic analysis may be used to derive analytic expressions for these numerical results. We multiply the PI equation in (7) by $y'(t)$ and integrate from $t = 0$ to $t = x$ and get

$$H \equiv \tfrac{1}{2}[y'(x)]^2 - 2[y(x)]^3 = \tfrac{1}{2}[y'(0)]^2 - 2[y(0)]^3 + I(x), \tag{11}$$

where $I(x) = \int_0^x dt\, t y'(t)$. The path of integration is the same as that used to calculate $y(t)$ numerically; the path follows the negative-real axis until it gets near a pole, at which point it makes a semicircular loop in the complex-t plane to avoid the pole.

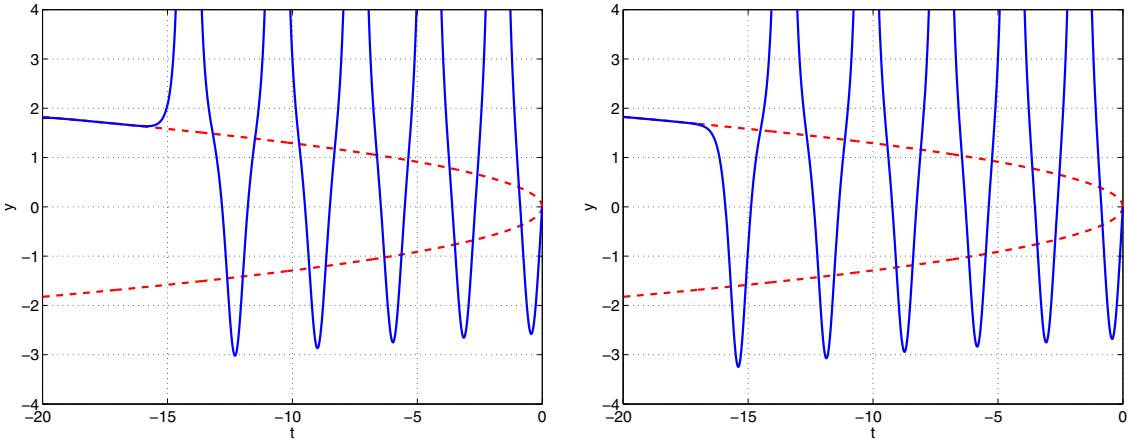

Figure 7. Tenth and eleventh eigenfunctions of Painlevé I with initial condition $y(0) = 0$. Left panel: $y'(0) = b_{10} = 8.244932302$. Right panel: $y'(0) = b_{11} = 8.738330156$. As n increases, the eigenfunctions pass through more double poles before exhibiting a turning-point-like transition and approaching the limiting curve $+\sqrt{-t/6}$ exponentially. This behavior is analogous to that of the eigenfunctions of a time-independent Schrödinger equation for a particle in a potential well; the higher-energy eigenfunctions exhibit many oscillations in the classically allowed region before entering the classically forbidden region, where they decay exponentially.

We calculate $I(x)$ for large-negative x in the classically allowed region (before the poles abruptly cease at the turning point) and find that on the real-x axis, as $n \to \infty$, $I(x)$ fluctuates and becomes small compared with H. This is not surprising because $I(x)$ receives many positive and negative contributions from the poles. We can see from the definition of $I(x)$ that $I'(x)$ vanishes when $y'(x)$ vanishes. Near the points where $y'(x)$ vanishes, we verify numerically that $I(x)$ is small compared with $-2[y(x)]^3$. Far from these points $y(x)$ becomes large, but so does $I(x)$. However, $-2[y(x)]^3$ blows up like a sixth-order pole and $I(x)$ blows up like a second-order pole. These asymptotic estimates are difficult to verify analytically, but numerical analysis confirms these results. These estimates are valid when x is large and negative but only in the classically allowed region and not as $x \to -\infty$.

By examining $I(x)$ as $x \to -\infty$, we can see a signal of an eigenvalue; as $y'(0) = b$ passes an eigenvalue, $I(x)$ goes from having positive to negative (or negative to positive) fluctuations, but at an eigenvalue $I(x)$ is smooth and does not fluctuate. For large n we treat the fluctuating quantity $I(x)$ as small and we interpret H as a time-independent quantum-mechanical Hamiltonian. [The isomonodromic properties of H when $I(x)$ is not neglected were studied in Ref. [62].]

To support these observations regarding the behavior of $I(x)$ on the real axis, we have done extremely detailed numerical studies of the distribution of poles and the behavior of PI in the complex-x plane. This gives a much clearer picture of the behavior of $I(x)$ for large x. We find that along the lines $x = re^{\pm i\pi/4}$, where r is real, the function $I(x)$ rapidly approaches 0 as $r \to \infty$. This provides strong evidence that the large-n (semiclassical) behavior of the eigenvalues is determined by solving the *linear* time-independent quantum-mechanical eigenvalue problem $\hat{H}\psi = E\psi$, where $\hat{H} = \frac{1}{2}\hat{p}^2 - 2\hat{x}^3$ along these lines in the complex-x plane. To find these eigenvalues we simply rotate $\hat{H}$ into the complex plane by $45^{c}irc$ [73] and obtain the well-studied $\mathcal{PT}$-symmetric Hamiltonian [2, 3]

$$\hat{H} = \tfrac{1}{2}\hat{p}^2 + 2i\hat{x}^3. \tag{12}$$

The large eigenvalues of this Hamiltonian are found by using the complex WKB techniques

discussed in Ref. [2]. For the class of $\mathcal{PT}$-symmetric Hamiltonians $\hat{H} = \frac{1}{2}\hat{p}^2 + g\hat{x}^2\,(i\hat{x})^\varepsilon$ $(\varepsilon \geq 0)$, the WKB approximation to the nth eigenvalue $(n \gg 1)$ is given by

$$E_n \sim \frac{1}{2}(2g)^{2/(4+\varepsilon)} \left[\frac{\Gamma\left(\frac{3}{2} + \frac{1}{\varepsilon+2}\right)\sqrt{\pi}\,n}{\sin\left(\frac{\pi}{\varepsilon+2}\right)\Gamma\left(1 + \frac{1}{\varepsilon+2}\right)} \right]^{(2\varepsilon+4)/(\varepsilon+4)}. \tag{13}$$

For H in (12) we take $g = 2$ and $\varepsilon = 1$ and obtain the asymptotic behavior

$$E_n \sim 2\left[\sqrt{3\pi}\Gamma\left(\tfrac{11}{6}\right) n/\Gamma\left(\tfrac{1}{3}\right)\right]^{6/5} \quad (n \to \infty). \tag{14}$$

The Hamiltonian $\hat{H}$ in (12) is time independent, so we evaluate H in (11) for fixed $y(0)$ and large $y'(0) = b_n$ and obtain the result

$$b_n \sim \sqrt{2E_n} = B_{\rm I} n^{3/5} \quad (n \to \infty), \tag{15}$$

which verifies (9). We read off the analytic value of the constant $B_{\rm I}$:

$$B_{\rm I} = 2\left[\sqrt{3\pi}\Gamma\left(\tfrac{11}{6}\right)/\Gamma\left(\tfrac{1}{3}\right)\right]^{3/5}, \tag{16}$$

which agrees with the numerical result in (9). Also, if we take the initial slope $y'(0)$ to vanish and take the initial condition $y(0) = c_n$ to be large, we obtain an analytic expression for $C_{\rm I}$,

$$C_{\rm I} = -\left[\sqrt{3\pi}\Gamma\left(\tfrac{11}{6}\right)/\Gamma\left(\tfrac{1}{3}\right)\right]^{2/5}, \tag{17}$$

which verifies (10). These analytic results are in precise agreement with our numerical work on the large-n behavior of the eigenvalues.

To obtain analytic expressions for $B_{\rm II}$ in (10) and $C_{\rm II}$ in (10), we follow the same procedure as for PI. We multiply the PII equation by $y'(t)$ and integrate from $t = 0$ to $t = x$, where x is in the turning-point region (where the simple poles stop). The result is

$$H \equiv \tfrac{1}{2}[y'(x)]^2 - \tfrac{1}{2}[y(x)]^4 = \tfrac{1}{2}[y'(0)]^2 - \tfrac{1}{2}[y(0)]^4 + I(x), \tag{18}$$

where $I(x) = \int_0^x dt\, t y(t) y'(t)$. The path of integration follows the negative-real axis until it gets near a simple pole, at which point it makes a loop in the complex-t plane to avoid the pole. As before, along this path the integrand of $I(x)$ oscillates and because of cancellations we neglect $I(x)$ when n is large.

We treat H as the $\mathcal{PT}$-symmetric quantum-mechanical Hamiltonian

$$\hat{H} = \tfrac{1}{2}\hat{p}^2 - \tfrac{1}{2}\hat{x}^4 \tag{19}$$

and use (13) with $g = 1/2$ and $\epsilon = 2$ to obtain

$$E_n \sim \tfrac{1}{2}\left[3n\sqrt{2\pi}\Gamma\left(\tfrac{3}{4}\right)/\Gamma\left(\tfrac{1}{4}\right)\right]^{4/3} \tag{20}$$

for the large eigenvalues of $\hat{H}$. For the eigenvalues b_n we use

$$\sqrt{2E_n} \sim \left[3n\sqrt{2\pi}\Gamma\left(\tfrac{3}{4}\right)/\Gamma\left(\tfrac{1}{4}\right)\right]^{2/3} \quad (n \to \infty) \tag{21}$$

from which we identify the value of $B_{\rm II}$:

$$B_{\rm II} = \left[3\sqrt{2\pi}\Gamma\left(\tfrac{3}{4}\right)/\Gamma\left(\tfrac{1}{4}\right)\right]^{2/3}. \tag{22}$$

To calculate C_{II} we note that the initial value $y(0)$ is positive. If we neglect $I(x)$ and assume a vanishing initial slope, we see that the right side of (18) is negative. Thus, as we did for the cubic Hamiltonian $\frac{1}{2}\hat{p}^2 - 2\hat{x}^3$, we perform a complex rotation of the coupling constant to convert the quartic Hamiltonian to $\hat{H} = \frac{1}{2}\hat{p}^2 + \frac{1}{2}\hat{x}^4$. Here, we obtain the conventional Hermitian quartic-anharmonic-oscillator Hamiltonian, which does not belong to the class of $\mathcal{PT}$-symmetric Hamiltonians $\hat{H} = \frac{1}{2}\hat{p}^2 + g\hat{x}^2(i\hat{x})^\epsilon$. The WKB approximation gives the large-eigenvalue approximation

$$E_n \sim \left[3n\sqrt{\pi}\Gamma\left(\tfrac{3}{4}\right)/\Gamma\left(\tfrac{1}{4}\right)\right]^{4/3} \quad (n \to \infty) \tag{23}$$

from which we read off the value of C_{II}:

$$C_{II} = \left[3\sqrt{\pi}\Gamma\left(\tfrac{3}{4}\right)/\Gamma\left(\tfrac{1}{4}\right)\right]^{1/3}. \tag{24}$$

To summarize, we have found the remarkable result that the large-eigenvalue behavior of PI, PII, and PIV (not discussed here) are obtained by WKB analysis of (1) for $\varepsilon = 1$, 2, 4. (We are planning further studies of PIII, PV, and PVI.) Finally, we note that the asymptotic analysis performed in this section has recently been verified at a more rigorous level [74].

5. Instabilities beyond the Painlevé transcendents

Let us consider a new class of nonlinear-differential-equation eigenvalue problems of the form

$$y''(x) = \frac{2M+2}{(M-1)^2}[y(x)]^M + x[y(x)]^N, \tag{25}$$

where M and N are integers. We refer to the members of this class as SP(M, N) (SP stands for super-Painlevé). These equations are a natural generalization of the first two Painlevé equations; PI in (4) is SP$(2, 0)$ and PII in (5) is SP$(3, 1)$. These equations give particularly interesting nonlinear eigenvalue problems when $N < M - 1$.

This special class of equations appear to have algebraic but not logarithmic movable singularities. To see why this is so recall that the solution to PI can become singular at an arbitrary point $x = A$ and the leading asymptotic approximation to such a solution is $y(x) \sim (x - A)^{-2}$ $(x \to A)$. However, to show that the singularity at $x = A$ is a pole it is necessary to show that an expansion around $x = A$ is a Laurent series. To do this we substitute

$$y(x) = \frac{1}{(x-A)^2}\left[1 + \sum_{n=1}^{\infty} a_n (x-A)^n\right] \tag{26}$$

into (4) and collect powers of $(x - A)$. If we solve recursively for the coefficients a_n, we find that the first five coefficients are $a_1 = 0$, $a_2 = 0$, $a_3 = 0$, $a_4 = -A/10$, and $a_5 = -1/6$. However, the key result is that a_6 is *undetermined* and thus is *arbitrary*. Since the series expansion for $y(x)$ contains *two arbitrary constants*, A and a_6, it follows that this series is the most general solution to the PI equation. To complete the argument one must show that the series expansion for $y(x)$ converges when $|x - A|$ is sufficiently small. This establishes that the expansion (26) is a Laurent series and verifies that the solutions to PI are meromorphic.

This analysis extends to the SP(M,N) equation, whose solutions can become singular at a point $x = A$. These singular solutions have the leading asymptotic behavior

$$y(x) \sim (x-A)^{-2/(M-1)} \quad (x \to A). \tag{27}$$

For simplicity, we study solutions that remain real on both sides of this singularity, so we assume that M is an *even* integer or $(M-1)/2$ is an odd integer. We seek an asymptotic expansion of $y(x)$ about the point $x = A$ of the form $y(x) = (x-A)^{-2/(M-1)}\left[1 + \sum_{n=1}^{\infty} a_n (x-A)^{1/(M-1)}\right]$. (This expansion is actually valid for both even and odd M; for odd M half of the terms vanish.) We substitute this expansion into the SP(M,N) equation and compare like powers of $x - A$ to find the coefficients, we see that the a_n are uniquely determined up to $n = 2(M+1)$ for even M and $n = M+1$ for odd M; at this value of n the coefficient a_n is *arbitrary*. Note that if $N \geq M-1$, the a_n term contains logarithmic terms.

As an example, we consider SP$(4,0)$. Here, the first seven coefficients vanish $a_1 = a_2 = a_3 = a_4 = a_5 = a_6 = a_7 = 0$ and the next two coefficients are $a_8 = -9A/22$ and $a_9 = 0$. Next, we find that a_{10} is *not determined and thus is arbitrary*. The next few coefficients are $a_{11} = 9/14$, $a_{12} = a_{13} = a_{14} = a_{15} = 0$, $a_{16} = 405A^2/4598$, $a_{17} = 0$. From here on the coefficients depend on the choice of a_{10}: $a_{18} = -45Aa_{10}/154$, $a_{19} = -135A/847$, $a_{20} = 6a_{10}^2/23$, $a_{21} = 45a_{10}/154$, and so on. We have found the general solution because the series contains two arbitrary constants, namely A and a_{10}. We do not present a proof here, but numerical analysis shows that the coefficients in the series have only geometric growth for large n, so the radius of convergence of the series is nonzero. While the series (27) is not a Laurent series because it contains fractional powers of $(x-A)$, our analysis shows that the solutions to the class of equations SP(M,N) have only algebraic singularities, and because M is chosen to be even, we may seek solutions that are entirely real. In particular, we can seek eigenfunction (separatrix) solutions that are real.

Solutions to the SP(M,N) equation have one or two possible real asymptotic behaviors as $x \to -\infty$: $y(x) \sim \pm\left[-(M-1)^2 x/(2M+2)\right]^{1/(M-N)}$. (There are two possible asymptotic curves when $M-N$ is even but only one when $M-N$ is odd.) As in the PI case, the upper curve is unstable and the lower curve is stable. Thus, the discrete eigenfunction (separatrix) solutions approach the upper curve. Here, we only consider here eigenfunction solutions for which $y(0) = 0$. The eigenvalues E_n are the initial values of the slope $y'(0)$ that give rise to solutions that approach the upper curve. For example, for $M = 4$ and $N = 2$, the first eight eigenvalues are 2.4240, 4.5364, 6.2471, 7.7792, 9.1960, 10.5292, 11.7973, 13.0127.

The analysis used for the Painlevé equations shows that if we neglect the function $I(x)$, we can replace the SP(M,N) equation by a simpler equation generated by the *linear* Hamiltonian

$$\hat{H} = \tfrac{1}{2}\hat{p}^2 + \tfrac{2}{(M-1)^2}\hat{x}^{M+1}.$$

In this approximation the term containing the parameter N has dropped out. The WKB formula (4) implies that for large n, the nth eigenvalue of $\hat{H}$ grows like $n^{(2M+2)/(M+3)}$ as $n \to \infty$. Thus, the nth separatrix eigenvalue $y'(0)$ grows like

$$y'(0) \sim n^{(M+1)/(M+3)} \quad (n \to \infty). \tag{28}$$

Our preliminary numerical studies show that (28) holds in some but not all cases. For $M = 4$ we expect the large-n behavior $n^{5/7}$ and for $M = 6$ we expect the behavior $n^{7/9}$. For $M = 4$ and $N = 2$ and for $M = 6$ and $N = 4$ this is what we find. Specifically, when $M = 4$, there are no eigenfunctions for $N = 0$, a full set of eigenfunctons qualitatively identical to those shown in Figs. 5-7 for $N = 1$, and a half-set of eigenfunctions qualitatively identical to those shown in the right panels of Figs. 5 and 6 and the left panel of Fig. 7 when $N = 2$. For the case $N = 2$

the eigenvalues grow like $n^{5/7}$. However, when $N = 1$, the eigenvalues grow slightly less rapidly; the nth eigenvalue grows like an^b, where $a = 2.04$ and $b = 0.56$.

When, $M = 6$, there is a half-set of eigenfunctions when $N = 0$ and no eigenfunctions when $N = 1$. However, when $N = 2$, $N = 3$, and $N = 4$, there are full sets of eigenfunctions. For the case $N = 4$ the eigenvalues grow like $n^{7/9}$, but when $N < 4$, the eigenvalues grow slightly less rapidly. Interestingly, it is the *largest* value of N that gives an eigenspectrum whose asymptotic behavior is determined by a linear approximation in which the y^N term in the nonlinear equation can be neglected! Evidently, for smaller values of N, the y^N term cannot be neglected. Specifically, when $N = 0$, the nth eigenvalue grows like $2.43n^{0.41}$; when $N = 2$, the nth eigenvalue grows like $2.55n^{0.54}$; when $N = 3$, the nth eigenvalue grows like $1.69n^{0.65}$. However, when $N = 4$, the nth eigenvalue grows like $3.06n^{7/9}$.

We have demonstrated that there is a huge, rich, and remarkable class of nonlinear-differential-equation eigenvalue problems for which there exists an infinite discrete set of eigenvalues. These differential equations are generalizations of the Painlevé transcendents. In full generality, the differential equations resulting from extending PI and PII have the form

$$y''(x) = \frac{2M+2}{(M-1)^2}[y(x)]^M + xP(y) + Q(y),$$

where $P(y)$ and $Q(y)$ are polynomials in $y(x)$ of degree less than $M - 1$. Clearly, there are additional general classes of nonlinear eigenvalue problems beyond the Painlevé transcendents. These new kinds of problems warrant much intensive further analysis.

Acknowledgments
I thank my colleagues A. Fring, J. Komijani, and Q. Wang for their contributions to our research on nonlinear eigenvalue problems.

References

[1] Bender C M 2015 $\mathcal{PT}$-symmetric quantum theory *J. Phys. Conf. Series* **631** 012002 [Talk given at the 4th Symposium on Prospects in the Physics of Discrete Symmetries (DISCRETE2014).]
[2] Bender C M and Boettcher S 1998 Real spectra in non-Hermitian Hamiltonians having $\mathcal{PT}$ symmetry *Physical Review Letters* **80** 5243-5246
[3] Bender C M (2007) Making Sense of Non-Hermitian Hamiltonians *Rep. Prog. Phys.* **70** 947-1018
[4] Guo A, Salamo G J, Duchesne D, Morandotti F, Volatier-Ravat M, Aimez V, Siviloglou G A and Christodoulides D N 2009 Observation of $\mathcal{PT}$-symmetry breaking in complex optical potentials *Phys. Rev. Lett.* **103** 093902
[5] Longhi S 2009 Bloch oscillations in complex crystals with $\mathcal{PT}$ symmetry *Phys. Rev. Lett.* **103** 123601
[6] Rüter C E, Makris, El-Ganainy R, Christodoulides D N, Segev M and Kip D 2010 Observation of $\mathcal{PT}$ symmetry in optics *Nat. Phys.* **6** 192
[7] Longhi S 2010 Optical realization of relativistic non-Hermitian quantum mechanics *Phys. Rev. Lett.* **105** 013903
[8] Lin Z, Ramezani H, Eichelkraut T, Kottos T, Cao H and Christodoulides D N 2011 Unidirectional invisibility induced by $\mathcal{PT}$-symmetric periodic structures *Phys. Rev. Lett.* **106** 213901
[9] Feng L, Ayache M, Huang J, Xu Y-L, Lu M-H, Chen Y-F, Fainman Y and Scherer A 2011 Nonreciprocal light propagation in a silicon photonic circuit *Science* **333** 729
[10] Ramezani H, Christodoulides D N, Kovanis V, Vitebskiy I and Kottos T 2012 $\mathcal{PT}$-symmetric Talbot effects *Phys. Rev. Lett.* **109** 033902
[11] Regensberger A, Bersch C, Miri M-A, Onishchukov G and Christodoulides D N 2012 Parity-time synthetic photonic lattices *Nature* **488** 167
[12] Razzari L and Morandotti R 2012 Gain and loss mixed in the same cauldron *Nature* **488** 163
[13] Liang G Q and Chong Y D 2013 Optical resonator analog of a two-dimensional topological insulator *Phys. Rev. Lett.* **110** 203904
[14] Luo X, Huang J, Zhong H, Qin X, Xie Q, Kivshar Y S and C Lee C 2013 Pseudo-parity-time symmetry in optical systems *Phys. Rev. Lett.* **110** 243902

[15] Regensberger A, Miri M-A, Bersch C, Nager J, Onishchukov G, Christodoulides D N and Peschel U 2013 Observation of defect states in $\mathcal{PT}$-symmetric optical lattices *Phys. Rev. Lett.* **110** 223902
[16] Hang C, Huang G and Konotop V V 2013 $\mathcal{PT}$ symmetry with a system of three-level atoms *Phys. Rev. Lett.* **110**, 083604
[17] Zheng C, Hao L and Long G L 2013 Observation of a fast evolution in a parity-time-symmetric system *Phil. Trans. R. Soc.* A **371** 20120053
[18] Rubinstein J, Sternberg P and Ma Q 2007 Bifurcation diagram and pattern formation of phase slip centers in superconducting wires driven by electric currents *Phys. Rev. Lett.* **99** 167003
[19] Chtchelkatchev N, Golubov A, Baturina T and Vinokur V 2012 Stimulation of the fluctuation superconductivity by $\mathcal{PT}$ symmetry *Phys. Rev. Lett.* **109** 150405
[20] Dietz B, Harney H L, Kirillov O N, Miski-Oglu M, Richter A and Schäfer F 2011 Exceptional points in a microwave billiard with time-reversal invariance violation *Phys. Rev. Lett.* **106** 150403
[21] Bittner S, Dietz B, Günther U, Harney H L, Miski-Oglu M, Richter A and Schäfer F 2012 $\mathcal{PT}$ symmetry and spontaneous symmetry breaking in microwave billiards *Phys. Rev. Lett.* **108** 024101
[22] Chong Y D, Ge L and Stone A D 2011 $\mathcal{PT}$-symmetry breaking and laser-absorber modes in optical scattering systems *Phys. Rev. Lett.* **106** 093902
[23] Liertzer M, Ge L, Cerjan A, Stone A D, Tureci H and Rotter S 2012 Pump induced exceptional points in lasers *Phys. Rev. Lett.* **108** 173901
[24] Zhao K F, Schaden M and Wu Z 2010 Enhanced magnetic resonance signal of spin-polarized Rb atoms near surfaces of coated cells *Phys. Rev.* A **81** 042903
[25] Schindler J, Li A, Zheng M C, Ellis F M and Kottos T 2011 Experimental study of active LRC circuits with $\mathcal{PT}$ symmetries *Phys. Rev.* A **84** 040101(R)
[26] Bender N, Factor S, Bodyfelt J D, Ramezani H, Christodoulides D N, Ellis F M and Kottos T 2013 Observation of asymmetric transport in structures with active nonlinearities *Phys. Rev. Lett.* **110** 234101
[27] Schomerus H 2010 Quantum noise and self-sustained radiation of $\mathcal{PT}$-symmetric systems *Phys. Rev. Lett.* **104** 233601
[28] West C T, Kottos T and Prosen T 2010 $\mathcal{PT}$-symmetric wave chaos *Phys. Rev. Lett.* **104** 054102
[29] Bender C M, Berntson B, Parker D and Samuel E 2013 Observation of $\mathcal{PT}$ phase transition in a simple mechanical system *Am. J. Phys.* **81** 173
[30] Fagotti M, Bonatti C, Logoteta D, Marconcini P and Macucci M 2011 Armchair graphene nanoribbons: $\mathcal{PT}$-symmetry breaking and exceptional points without dissipation *Phys. Rev.* B **83** 241406(R)
[31] Szameit A, Rechtsman M C, Bahat-Treidel O and Segev M 2012 $\mathcal{PT}$-symmetry in honeycomb photonic lattices *Phys. Rev.* A **84** 021806
[32] Bender C M, Gianfreda M, Peng B, Özdemir S K and Yang L 2013 Twofold transition in $\mathcal{PT}$-symmetric coupled oscillators *Phys. Rev.* A **88** 062111
[33] Peng B, Özdemir S K, Lei F, Monifi F, Gianfreda M, Long G L, Fan S, Nori F, Bender C M and Yang L 2014 Parity-time-symmetric whispering-gallery microcavities *Nature Physics* **10** 394
[34] Peng B, Özdemir S K, Rotter S, Yilmaz H, Liertzer M, Monifi F, Bender C M, Nori F and Yang L 2014 Loss-induced suppression and revival of lasing *Science* **346**, 328
[35] Cartarius H and Wunner G 2012 Model of a $\mathcal{PT}$-symmetric Bose-Einstein condensate in a δ-function double-well potential *Phys. Rev.* A **86** 013612
[36] Kreibich M, Main J, Cartarius H and Wunner G (2013) Hermitian four-well potential as a realization of a $\mathcal{PT}$-symmetric system *Phys. Rev.* A **87** 051601
[37] Kartashov Y V, Konotop V V and Abdullaev F Kh 2013 Gap solitons in a spin-orbit-coupled Bose-Einstein condensate *Phys. Rev. Lett.* **111** 060402
[38] Castaldi G, Savoia S, Galdi V, Alu A and Engheta N 2013 $\mathcal{PT}$ metamaterials via complex coordinate transformation optics *Phys. Rev. Lett.* **110** 173901
[39] Lazarides N and Tsironis G P 2013 Gain-driven discrete breathers in $\mathcal{PT}$-symmetric nonlinear metamaterials *Phys. Rev. Lett.* **110** 053901
[40] Yin X and Zhang X 2013 Unidirectional light propagation at exceptional points *Nature Materials* **12** 175
[41] Feng L, Xu Y-L, Fegadolli W S, Lu M-H, Oliveira J E B, Almeida V R, Chen Y-F and Scherer A 2013 Experimental demonstration of a unidirectional reflectionless parity-time metamaterial at optical frequencies *Nature Materials* **12** 108
[42] Dorey P E, Dunning C, and Tateo R (2001) Spectral equivalences, Bethe ansatz equations, and reality properties in PT-symmetric quantum mechanics *J. Phys. A: Math. Gen.* **34**, 5679
[43] Dorey P E, Dunning C, and Tateo R (2007) The ODE/IM Correspondence *J. Phys. A: Math. Theor.* **40**, R205
[44] Ahmed Z, Bender C M, Berry M V (2005) Reflectionless Potentials and $\mathcal{PT}$ Symmetry *J. Phys. A: Math. Gen.* **38**, L627-L630

[45] Bender C M, Brody D C, Chen J-H, Jones H F, Milton K A, and Ogilvie M C (2006) Equivalence of a Complex $\mathcal{PT}$-Symmetric Quartic Hamiltonian and a Hermitian Quartic Hamiltonian with an Anomaly *Phys. Rev. D* **74**, 025016
[46] Bender C M, Moshe M, and Sarkar S (2013) $\mathcal{PT}$-symmetric interpretation of double-scaling *J. Phys. A: Math. Theor.* **46**, 102002
[47] Bender C M and Sarkar S (2013) Double-scaling limit of the O(N)-symmetric anharmonic oscillator *J. Phys. A: Math. Theor.* **46** 442001 (2013)
[48] Lee T D (1954) *Phys. Rev.* **95** 1329
[49] Källén G and Pauli W (1955) *Mat.-Fys. Medd.* **30**, No. 7
[50] Bender C M, Brandt S F, Chen J-H, and Wang Q (2005) Ghost Busting: $\mathcal{PT}$-symmetric interpretation of the Lee model *Physical Review D* **71** 025014
[51] Bender C M, Hook D W, Mavromatos N E, and Sarkar S (2016) $\mathcal{PT}$-symmetric interpretation of unstable effective potentials *J. Phys. A: Math. Theor.* **49** 45LT01
[52] Bender C M and Gianfreda M (2015) $\mathcal{PT}$-symmetric interpretation of the electromagnetic self-force *J. Phys. A: Math. Theor.* **48** 34FT01
[53] Bender C M, Fring A, and Komijani J (2014) Nonlinear eigenvalue problems *J. Phys. A: Math. Theor.* **47** 235204
[54] Kerr O S (2014) Comment on "Nonlinear eigenvalue problems" *J. Phys. A: Math. Theor.* **47** 368001 (2014)
[55] Bender C M and Komijani J (2015) Painlevé Transcendents and $\mathcal{PT}$-Symmetric Hamiltonians *J. Phys. A: Math. Theor.* **48** 475202
[56] Bender C M, Komijani J, and Wang Q (2017) Nonlinear eigenvalue problems *CRM Conference Series* (in press)
[57] Ince P L (1956) *Ordinary Differential Equations* (Dover, New York); Miles J W (1978) On the second Painlevé transcendent *Proc. Roy. Soc. London A* **361** 277-291; Holmes P and Spence D (1984) On a Painlevé-type boundary-value problem *Quart. J. Mech. Appl. Math.* **37** 525-538; Hastings S P and McLeod J B (2011) Classical methods in ordinary differential equations: With applications to boundary value problems *Graduate Studies in Math.* **129** (American Mathematical Society)
[58] A detailed study of the asymptotic behavior of the Painlevé transcendents may be found in Jimbo M and Miwa T (1981) *Physica D* **2** 407-448
[59] Separatrix behavior of the first Painlevé transcendent is mentioned briefly in Kapaev A A (1989) *Differential Equations* **24** 1107-1115; see also Kapaev A A (2002) Monodromy deformation approach to the scaling limit of the Painlevé first equation *CRM Proc. Lect. Notes* **32** 157-179
[60] Clarkson P A (2003) Painlevé Equations — Nonlinear special functions *J. Comp. Appl. Math.* **153** 127-140
[61] Maseoro P (2010) Essays on the Painlevé first equation and the cubic oscillator (PhD Thesis, SISSA)
[62] Kawai T and Takei Y (2005) Algebraic analysis of singular perturbation theory (American Mathematical Society, New York)
[63] Costin O, Costin R D, and Huang M (2013) Tronquée solutions of the Painlevé equation P_1 (unpublished)
[64] Fokas A S, Its A R, Kapaev A A, and Novokshonov V Y (2006) Painlevé transcendents: The Riemann-Hilbert approach (American Mathematical Society, New York)
[65] The spin-spin correlation function for the two-dimensional Ising model for temperatures near T_c is described by PIII. See Wu T T, McCoy B M, Tracy C A, and Barouch E (1976) Spin-spin correlation functions for the two-dimensional Ising model: exact theory in the scaling region *Phys. Rev. B* **13** 316-374
[66] For all temperatures the diagonal correlation function for the Ising model in two dimensions $\langle\sigma_{0,0}\sigma_{N,N}\rangle$ is given in terms of PVI. See Jimbo M and Miwa T (1980) Studies on holonomic quantum fields XVII *Proc. Jap. Acad.* **56A** 405 and (1981) **57A** 347
[67] Brézin E and Kazakov V A (1990) Exactly solvable field theories of closed strings *Phys. Lett. B* **236** 144-150
[68] Douglas M and Shenker S (1990) Strings in less than one dimension *Nucl. Phys. B* **335** 635-654
[69] Gross P and Migdal A (1990) A nonperturbative treatment of two-dimensional quantum gravity *Nucl. Phys. B* **340** 333-365
[70] Moore G (1990) Geometry of the string equations *Comm. Math. Phys.* **133** 261-304; Matrix models of 2D gravity and isomonodromic deformations *Prog. Theor. Phys. Suppl.* **102** 255-285
[71] Fokas A S, Its A R, and Kitaev A V (1992) The isomonodromy approach to matrix problems in 2D quantum gravity *Comm. Math. Phys.* **147** 395-430
[72] Bender C M and Orszag S A (1978) *Advanced Mathematical Methods for Scientists and Engineers* (McGraw Hill, New York), chap. 4
[73] See Reinhardt W P (1982) *Ann. Rev. Phys. Chem.* **33** 223 for a review of complex rotation of coordinates.
[74] Long W-G, Li Y-T, Liu S-Y, and Zhao Y-Q (2016) Real solutions of the first Painlevé equation with large initial data (arXiv:1612.01350 [math.CA])